

Continuous spectra of a family of lattices containing the modified rectangle lattice of Dhar

William A. Schwalm* and Brian J. Moritz

Physics Department, University of North Dakota, Grand Forks, North Dakota 58202, USA

(Received 20 January 2005; published 28 April 2005)

A large body of evidence has accumulated suggesting that the spectrum associated with linear wave dynamics on a typical finitely ramified, hierarchical structure should consist of a Cantor-like portion and a nested hierarchy of discrete eigenvalues lying in the gaps of the Cantor set. However, careful analysis of renormalization recursion relations of the discrete Schrödinger equation on this family of lattices associated with the modified rectangle lattice first introduced by Dhar shows that in the large lattice limit the spectra contain only a continuum with a smooth density of states. In addition, at random energy the Greenwood-Peierls conductance shows metallic behavior rather than tending to zero with increasing lattice size due to Anderson localization.

DOI: 10.1103/PhysRevB.71.134207

PACS number(s): 05.45.Df, 71.23.-k, 64.60.Ak, 73.90.+f

I. INTRODUCTION

We report a surprising case of a family of finitely ramified, hierarchical lattices with continuous spectra and smooth eigenvalue densities that show evidence of metallic conduction. We know of no other examples of a heterogeneous hierarchical lattice (i.e., ones in which local environments of individual sites are essentially different for all sites modulo a trivial point symmetry of the overall lattice) in which the eigenvalue spectrum contains a continuum. Moreover, it is shown below that for a certain energy range the modified rectangle lattice has a nonvanishing Greenwood-Peierls conductance sum for the case of one-dimensional lead wires attached to distal points on a finite portion lattice, even in the limit that the lattice diameter goes to infinity. The existence of a spectral continuum and nonvanishing conductance sum appears to contradict what one would expect for any such lattice.

In the recent past, models of linear wave dynamics on fractal or hierarchical lattices have received quite a bit of attention primarily for two reasons: (i) These models renormalize exactly and hence can be studied in great detail and (ii) they may relate to random systems, such as percolation clusters or amorphous materials.¹⁻⁴ One early example to appear was the modified rectangle lattice presented by Dhar¹ (see Fig. 1) at about the same time that he introduced the 2-simplex lattice.²

The 2-simplex lattice (essentially the Sierpiński lattice^{3,4}) is a prototype for a family of finitely ramified, hierarchical lattices that are often fractals. On these lattices the local bonding geometry or site environment is basically different from site to site (modulo a trivial point symmetry). For example, each site on an infinite Sierpiński lattice is adjacent to three triangular faces of varying size. As more and more sensitive measures of local symmetry are employed, more and more individuality is detected. This is expected to contribute to reflected waves of incommensurate wave lengths and thus induce wave localization.⁵ Therefore, one expects (and almost always finds) Anderson localization⁶ in the regular, finitely ramified hierarchical models because of this incommensurate superposition due to the fluctuating site envi-

ronment. In this way these models can be compared roughly to the more complicated random models.

The dynamical and spectral properties of linear wave models are thoroughly studied for quite a large number of finitely ramified, hierarchical structures. Most follow the general pattern of the 2-simplex case: the spectrum consists of a Cantor-like portion with a sequence of isolated eigenvalues sitting in the gaps of the Cantor set.^{7,8} In the following we present a detailed study of linear wave dynamics on the modified rectangle lattice and its family. The spectra associated with the standard linear models on these structures each contain a continuum with a smooth density of states, more like that of a periodic structure or Bethe lattice⁹ than that of a fractal or other finitely ramified, hierarchical structure.

In Sec. II we introduce briefly the standard linear model and transfer-matrix renormalization method employed in this study. Section III contains a description of several members of the family of lattices related to the modified rectangle lattice of Dhar and includes the results of analyzing the renormalization recursions for these examples. In each case, the analysis yields a closed-form expression for the diagonal, pivotal Green function, in the large lattice limit, as a function of the dimensionless complex energy parameter $z = \varepsilon + i\eta$. The local density of states for each member of the family studied in Sec. III appears in Secs. IV and V presents the method and analysis extended to any member of the family. Section VI includes a discussion of the Kubo-Greenwood conductance for the modified rectangle lattice, and the paper concludes with a brief discussion of the results and the curious properties of this family of hierarchical lattices.

II. THE MODEL

Linear models for lattice vibrations, spin waves or Schrödinger dynamics of independent electrons are all really the same model, so we present our study in terms of the discrete Schrödinger equation, which also facilitates the computation of quantum conductance. The energy is scaled in terms of the hopping matrix element so the graph adjacency matrix

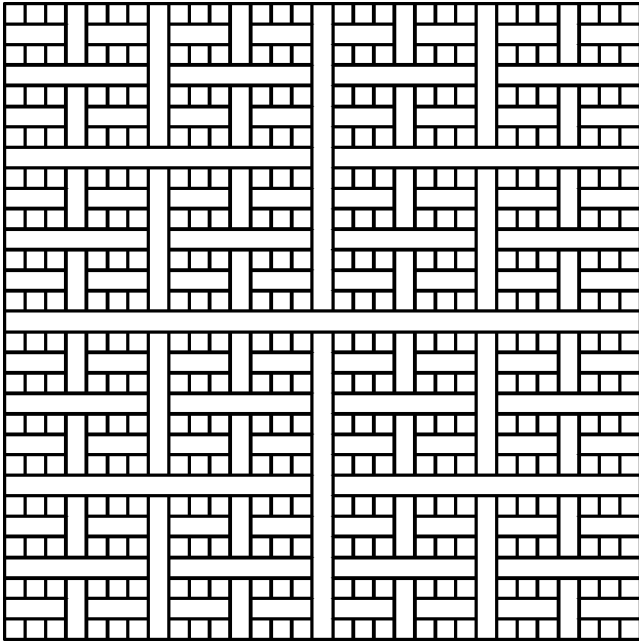


FIG. 1. Modified rectangle lattice, stage 9 in construction ($n=9$).

$$H_{ij} = \begin{cases} 1 & \text{if } i@j, \\ 0 & \text{otherwise,} \end{cases} \quad (1)$$

serves as a model Hamiltonian, where the notation $i@j$ indicates that sites i and j of a lattice belong to the same bond. The discrete Laplacian is $\nabla^2 = H - 3$, making the dimensionless effective mass negative and in the following discussion the ground state (where wave amplitudes are all of the same sign) has the highest eigenvalue rather than the lowest. Since the lattice is regular and bipartite, the spectrum is symmetric about $z=0$, so the sign of the effective mass can be ignored.

We employ the standard transfer-matrix renormalization method.^{5,10} The retarded Green function $\hat{G}_{ij}(t)$ for the discrete Schrödinger equation is a matrix element of $\hat{G}(t)$ satisfying

$$i \frac{d}{dt} \hat{G}(t) - H \hat{G}(t) = I \delta(t), \quad (2)$$

with $\hat{G}(t) = \theta(t) \hat{G}(t)$. The Fourier transform gives the resolvent

$$g(z) = (z - H)^{-1}, \quad (3)$$

defined for z outside the spectrum of H . The local density of states projected on site j is given by

$$D_j(\varepsilon) = -\frac{1}{\pi} \text{Im} \langle j | g(\varepsilon + i\eta) | j \rangle. \quad (4)$$

The Kubo-Greenwood electrical conductance between one-dimensional leads attached at sites i and j is simply related to $g_{ii}(z)$, $g_{ij}(z)$ and $g_{jj}(z)$.

Examples of the recursive construction of a lattice are illustrated in Figs. 2–4. Consider forming the generation- n

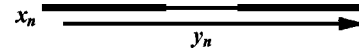


FIG. 2. Recursive construction of the linear chain as a hierarchical lattice and definition of the pivotal Green functions x_n and y_n .

graph. The graph matrix representing two identical, disconnected generation- $(n-1)$ graphs is the direct sum,

$$H_o^{(n)} = H^{(n-1)} \oplus H^{(n-1)}. \quad (5)$$

Additional connections shown in Fig. 3(a) correspond to the addition of a sparse connection matrix V such that

$$H^{(n)} = H_o^{(n)} + V. \quad (6)$$

Using lower case for generation $n-1$ and uppercase for n ,

$$g(z) = (z - H^{(n-1)})^{-1}, \quad (7)$$

$$G(z) = (z - H^{(n)})^{-1}. \quad (8)$$

Matrix algebra yields the standard result

$$G(z) = g(z) + g(z)VG(z). \quad (9)$$

For each n , V always has a small, fixed number of nonzero entries. One studies physical properties as a function of the energy parameter z and generation number n using a small pivotal set of Green functions and the recursion relations obtained from Eq. (9).

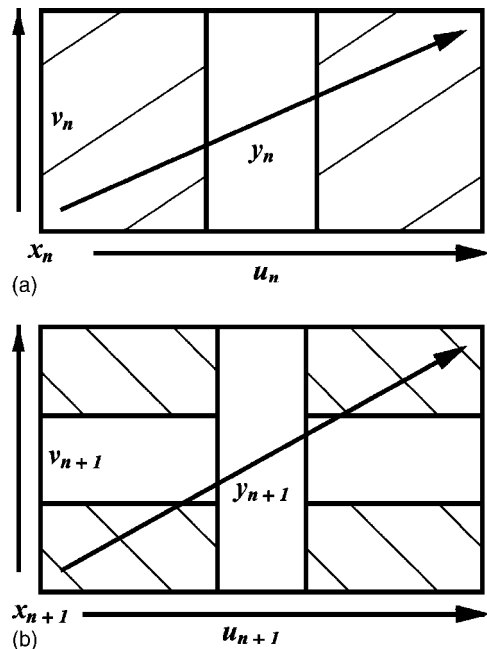


FIG. 3. Block connections and definition of Green functions for the modified rectangle lattice for successive generations n and $n+1$ using generation $n-1$ blocks: (a) generation n constructed from two-generation $n-1$ blocks and (b) generation $n+1$ constructed from two-generation n blocks as shown in Fig. 3(a).

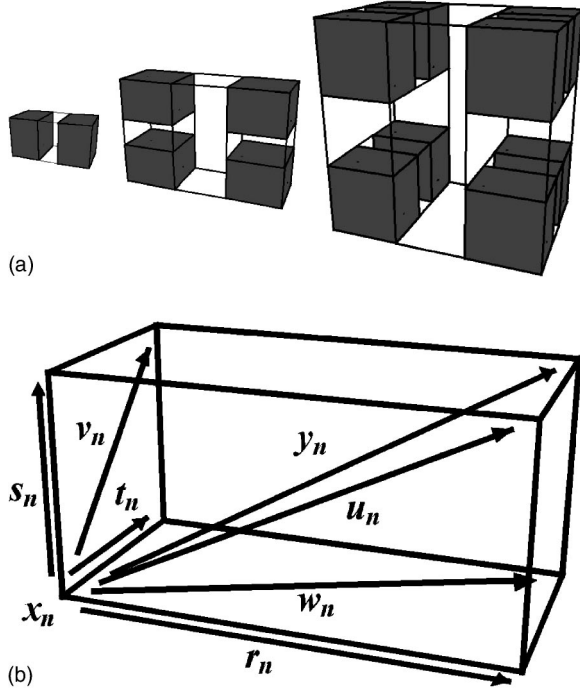


FIG. 4. Recursive construction for the modified cubic lattice and graphical definition of the 8 pivotal Green functions: (a) three successive generations of the modified cubic lattice and (b) pivotal Green function definitions for generation n .

III. GREEN FUNCTION RECURSIONS OF THE MODIFIED RECTANGLE LATTICE AND RELATED FAMILY

A. Linear chain

The first member of the family that we describe is the linear chain, which has been studied extensively. The recursive construction and pivotal set are shown in Fig. 2. The recursion relations obtained from Eq. (9) reduce modulo the point group¹⁰ C_2 that is isomorphic to Z_2 with

$$p = x + y, \quad q = x - y. \quad (10)$$

The symmetry-reduced recursions are

$$P = \frac{2pq - p - q}{p + q - 2}, \quad Q = \frac{2pq + p + q}{p + q + 2}. \quad (11)$$

Prior to analyzing dynamical behavior we reduce the order of the recursions by transforming to canonical variables¹¹ obtained by finding a Lie group that commutes with the renormalization map as described by Maeda.¹² Studying the fixed and invariant manifolds¹³ of Eqs. (11) a set of canonical coordinates is

$$a = \frac{p+1}{p-1}, \quad b = \frac{(p-1)(q+1)}{(p+1)(q-1)}. \quad (12)$$

Further reduction comes by transforming from a to the invariant

$$\delta = a^2 b, \quad (13)$$

from which the dynamical system reduces to

$$\Delta = \delta, \quad B = \frac{4b}{(b+1)^2}, \quad (14)$$

with initial conditions

$$\delta_o = \frac{z+2}{z-2}, \quad b_o = \frac{z-2}{z+2}. \quad (15)$$

After studying the orbits of the initial conditions for z outside the spectral range $-2 \leq z \leq 2$, we find the correct form for the pivotal Green function $x_{lc}(z)$ in the large lattice limit as

$$x_{lc}(z) = \frac{z - \sqrt{z-2}\sqrt{z+2}}{2}. \quad (16)$$

B. Modified rectangle

The recursive construction and pivotal set for the modified rectangle lattice are shown in Fig. 3. The recursion relations simplify modulo the point group¹⁰ D_2 of the rectangle that is isomorphic to $Z_2 \oplus Z_2$ with the symmetrized pivotal set

$$\begin{aligned} p &= x + y + u + v, & q &= x - y + u - v, \\ r &= x - y - u + v, & s &= x + y - u - v, \end{aligned} \quad (17)$$

and similar definitions for the pivotal set $\{P, Q, R, S\}$ on generation $n+1$. The symmetry-reduced recursions¹³ are

$$\begin{aligned} P &= \frac{2pq - p - q}{p + q - 2}, & Q &= \frac{2rs - r - s}{r + s - 2}, \\ R &= \frac{2pq + p + q}{p + q + 2}, & S &= \frac{2rs + r + s}{r + s + 2}. \end{aligned} \quad (18)$$

Note the similarity to the recursions obtained for the linear chain.

We reduce the order of the recursions by transforming to canonical variables following the example of the linear chain. The symmetry-reduced pivotal set is

$$\begin{aligned} a &= \frac{p+1}{p-1}, & b &= \frac{(p-1)(q+1)}{(p+1)(q-1)}, \\ c &= \frac{(p-1)(r+1)}{(p+1)(r-1)}, & d &= \frac{(p-1)(s+1)}{(p+1)(s-1)}. \end{aligned} \quad (19)$$

Further reduction comes from transforming from a to the invariant quantity

$$\delta = a^4 bcd. \quad (20)$$

Using the canonical coordinates $\{\delta, b, c, d\}$,

$$\Delta = \delta \quad (21)$$

and the dynamics are governed by the residual system

$$B = \frac{c+d}{b+1}, \quad C = \frac{4b}{(b+1)^2},$$

$$D = \frac{4cd}{(b+1)(c+d)}. \quad (22)$$

The initial conditions

$$\delta_o = \frac{(z+3)(z+1)}{(z-3)(z-1)},$$

$$b_o = d_o = \frac{z-3}{z+1}, \quad c_o = \frac{(z-3)(z+3)}{(z-1)(z+1)}, \quad (23)$$

come from computing the Green functions for a dimer or computing the Green functions for a unit square and backing up one step.

From Eqs. (17) and (19), the fixed point $(b, c, d) = (1, 1, 1)$ corresponds to $(y, u, v) = (0, 0, 0)$, indicating no electron propagation across the lattice. Orbits from (b_o, c_o, d_o) with z outside the spectral range $-3 \leq z \leq 3$ all iterate toward $(1, 1, 1)$. The Green function x is found in closed form in the large L limit using this fixed point and the invariance of δ . The correct expression for x in terms of $\{\delta, b, c, d\}$ is the only one of the four possible inverse transformations that gives the positive, smooth density of states shown in Fig. 5(b), namely,

$$x_{mr} = \frac{\sqrt[4]{\delta} - 1}{\sqrt[4]{\delta} + 1} = \frac{\sqrt[4]{\delta_o} - 1}{\sqrt[4]{\delta_o} + 1}, \quad (24)$$

in the limit that $(b, c, d) \rightarrow (1, 1, 1)$. In terms of z ,

$$x_{mr}(z) = \frac{\sqrt[4]{z+3}\sqrt[4]{z+1} - \sqrt[4]{z-3}\sqrt[4]{z-1}}{\sqrt[4]{z+3}\sqrt[4]{z+1} + \sqrt[4]{z-3}\sqrt[4]{z-1}}. \quad (25)$$

This is the explicit, closed-form solution for the pivotal Green function $x_{mr}(z)$ in the large lattice limit that $\sim 1/z$ as $z \rightarrow \infty$.

C. Modified cube

The final example is the modified cubic lattice that has not appeared previously in the literature. The recursive construction and pivotal set are defined in Fig. 4. The recursions obtained from Eq. (9) simplify by transforming to the symmetry-reduced combinations

$$a = x + y + r + s + t + u + v + w,$$

$$b = x - y + r + s - t + u - v - w,$$

$$c = x - y + r - s + t - u - v + w,$$

$$d = x + y + r - s - t - u + v - w,$$

$$e = x - y - r + s + t - u + v - w,$$

$$f = x + y - r + s - t - u - v + w,$$

$$g = x + y - r - s + t + u - v - w,$$

$$h = x - y - r - s - t + u + v + w, \quad (26)$$

obtained from the point-group symmetry of the cube isomorphic to $Z_2 \oplus Z_2 \oplus Z_2$. Using these combinations in the equations obtained from Eq. (9) and solving for the recursion relations in terms of the symmetrized pivotal set $\{a, b, c, d, e, f, g, h\}$ yields

$$A = \frac{2ab - a - b}{a + b - 2}, \quad B = \frac{2cd - c - d}{c + d - 2},$$

$$C = \frac{2ef - e - f}{e + f - 2}, \quad D = \frac{2gh - g - h}{g + h - 2},$$

$$E = \frac{2ab + a + b}{a + b + 2}, \quad F = \frac{2cd + c + d}{c + d + 2},$$

$$G = \frac{2ef + e + f}{e + f + 2}, \quad H = \frac{2gh + g + h}{g + h + 2}. \quad (27)$$

By the same Lie group technique used to reduce the recursions of the modified rectangle, the combinations

$$\delta = \frac{(a+1)(b+1)(c+1)(d+1)}{(a-1)(b-1)(c-1)(d-1)}$$

$$\times \frac{(e+1)(f+1)(g+1)(h+1)}{(e-1)(f-1)(g-1)(h-1)},$$

$$j = \frac{(a-1)(b+1)}{(a+1)(b-1)},$$

$$k = \frac{(a-1)(c+1)}{(a+1)(c-1)}, \quad l = \frac{(a-1)(d+1)}{(a+1)(d-1)},$$

$$m = \frac{(a-1)(e+1)}{(a+1)(e-1)}, \quad n = \frac{(a-1)(f+1)}{(a+1)(f-1)},$$

$$p = \frac{(a-1)(g+1)}{(a+1)(g-1)}, \quad q = \frac{(a-1)(h+1)}{(a+1)(h-1)}, \quad (28)$$

reduce the recursions to

$$\Delta = \delta,$$

$$J = \frac{k+l}{j+1}, \quad K = \frac{m+n}{j+1}, \quad L = \frac{p+q}{j+1},$$

$$M = \frac{4j}{(j+1)^2},$$

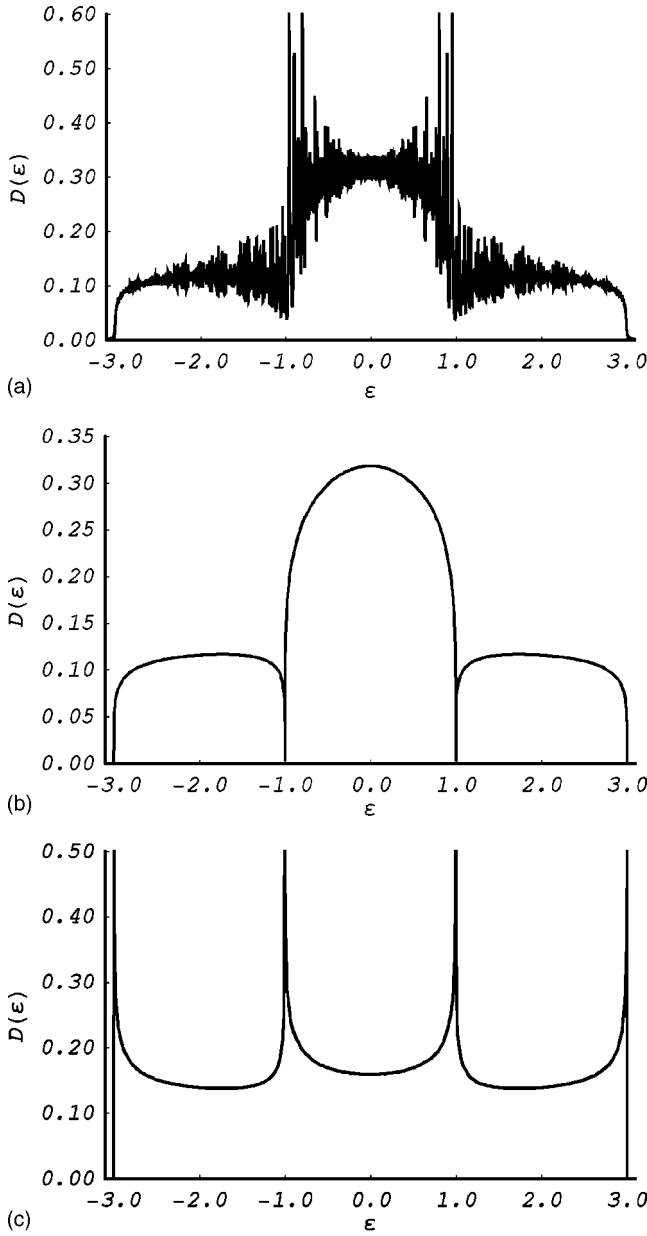


FIG. 5. Local density of states (states per site per unit energy) for the modified rectangle vs energy in units of the hopping matrix element: (a) LDOS for a corner site for generation $n=9$ in the construction of the modified rectangle ($\eta=0.005$), (b) LDOS for a corner site in the limit $L \rightarrow \infty$ and $\eta \rightarrow 0$ for the modified rectangle, and (c) LDOS for an $(n-1)$ bridge-point site in the large lattice of the modified rectangle ($n \rightarrow \infty$, $\eta \rightarrow 0$).

$$N = \frac{4kl}{(j+1)(k+l)},$$

$$P = \frac{4mn}{(j+1)(m+n)}, \quad Q = \frac{4pq}{(j+1)(p+q)}, \quad (29)$$

with initial conditions

$$\delta_o = \frac{(z+4)(z+2)^2}{(z-4)(z-2)^2},$$

$$j_o = l_o = n_o = q_o = \frac{z-4}{z},$$

$$k_o = m_o = \frac{(z-4)(z+2)}{z(z-2)},$$

$$p_o = \frac{(z-4)(z+4)}{z^2}. \quad (30)$$

The behavior of the Green functions in the large lattice limit can be used to derive an explicit expression for the corner-site, diagonal Green function $x_{mc}(z)$. For z outside the spectrum, each of the residual pivotal Green functions tend to 1 as $n \rightarrow \infty$ so that $(b, c, d, e, f, g, h) \rightarrow (0, 0, 0, 0, 0, 0, 0)$ in the large lattice limit. From Eqs. (28), the values of the pivotal Green functions in the large lattice limit and, substituting the initial condition for δ ,

$$x_{mc}(z) = \frac{8\sqrt{z+4}\sqrt[4]{z+2} - 8\sqrt{z-4}\sqrt[4]{z-2}}{8\sqrt{z+4}\sqrt[4]{z+2} + 8\sqrt{z-4}\sqrt[4]{z-2}}. \quad (31)$$

IV. LOCAL DENSITY OF STATES

The local density of states (LDOS) for a corner site is computed from Eq. (4) with $g_{jj}(\varepsilon + i\eta) = x_n(z)$ for a generation n lattice in the family. Starting with initial conditions and small positive η , the recursions Eqs. (14), (22) or (29) are iterated n times to obtain final values for the residual pivotal set that together with the invariant yield the correct $x_n(z)$. Figure 5(a) shows the resulting $D_{mr}(\varepsilon)$ for a finite-size modified rectangle lattice, $n=9$, and Fig. 5(b) shows the result obtained from Eq. (25). As the number of sites increases, $D(\varepsilon)$ for each member of the family becomes a smooth curve, characteristic of regular lattices (including the Bethe lattice) but very different from the spectrum of a typical finitely ramified, hierarchical lattice.^{7,8}

A. Linear chain

Although the linear chain is a member of this family because of the structure of its Green-function renormalization recursions, the linear chain is a regular lattice and its LDOS is well known. We include Fig. 6 for completeness. The Euclidian embedding dimension d , self-similarity or fractal dimension d_f and spectral dimension d_s are all equal to 1.

B. Modified rectangle

Figure 5 shows the local density of states for the modified rectangle lattice. Van Hove singularities exist at $\varepsilon = -3, -1, 1, 3$. The bond length between adjacent sites is held fixed for all generations in the recursive construction leading to a self-similarity dimension d_f (also the mass-scaling dimension) that is equal to the Euclidian embedding dimension d

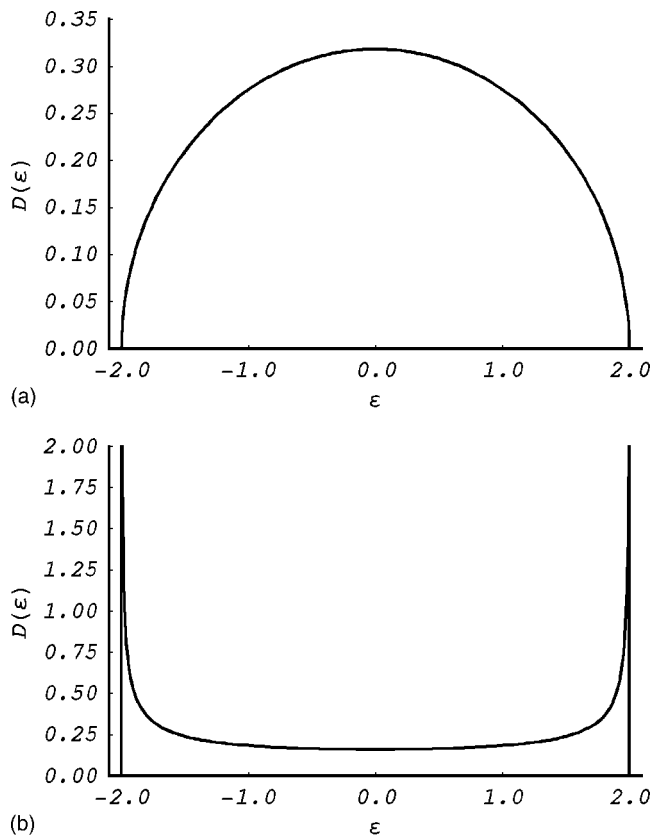


FIG. 6. Local density of states (states per site per unit energy) for the linear chain vs energy in units of the hopping matrix element: (a) LDOS for the site at the end of a semi-infinite chain and (b) LDOS for a site in the infinite linear chain.

$=2$. The total density of states $D_{mr}^{tot}(\epsilon)$ diverges near the ground state energy as

$$D_{mr}^{tot}(\epsilon) \sim |\epsilon - 3|^{-1/4}$$

for $\epsilon \rightarrow 3$. Thus, the spectral dimension^{14,15} of the modified rectangle lattice is $d_s = 3/2$. This result is equivalent to that obtained by Dhar¹ and also can be obtained by first determining the anomalous-diffusion exponent d_w from the conductivity exponent $\tilde{\mu}$ or resistance exponent $\tilde{\zeta}$ using the Einstein relation connecting the dc conductivity to the diffusion constant.^{14,16,17} An exact renormalization procedure⁴ gives the resistance exponent $\tilde{\zeta} = 2/3$ and, therefore, $d_w = 8/3$ yielding¹⁴

$$d_s = \frac{2d_f}{d_w} = \frac{3}{2}.$$

C. Modified cube

Figure 7 shows the local density of states for the modified cubic lattice. Van Hove singularities exist at $\epsilon = -4, -2, 2, 4$. As in the case of the modified rectangle, the bond length between adjacent sites is held fixed for all generations in the recursive construction leading to a self-similarity dimension that is equal to the Euclidian embedding dimension $d = 3$.

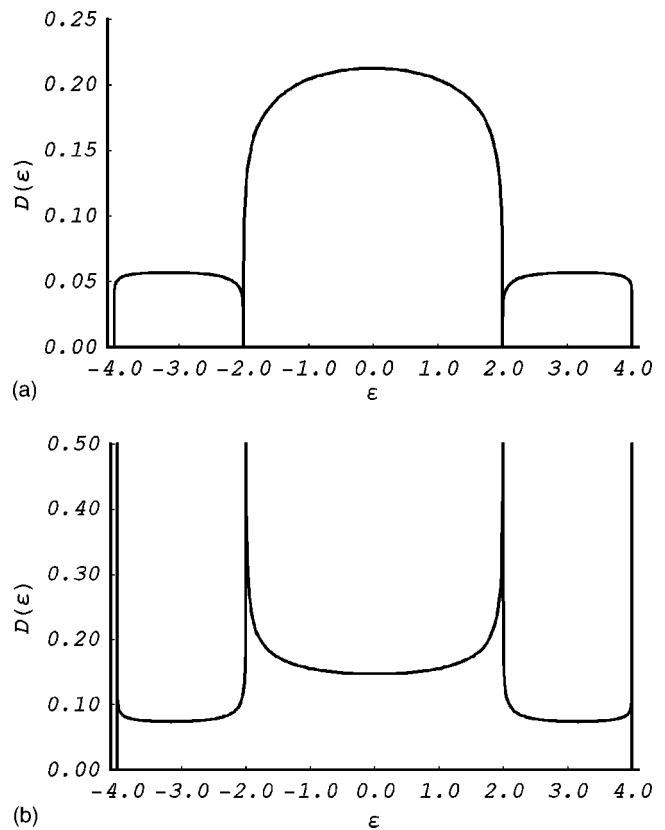


FIG. 7. Local density of states (states per site per unit energy for the modified cube vs energy in units of the hopping matrix element: (a) LDOS for a corner site in the limit $L \rightarrow \infty$ and $\eta \rightarrow 0$ for the modified cube and (b) LDOS for an $(n-1)$ bridge-point site in the large lattice limit of the modified cube ($n \rightarrow \infty, \eta \rightarrow 0$).

The total density of states diverges for $\epsilon \rightarrow 4$ as

$$D_{mc}^{tot}(\epsilon) \sim |\epsilon - 4|^{-1/8},$$

so that the spectral dimension $d_s = 7/4$ for the modified cubic lattice.

V. RESULTS FOR $d > 3$

The analysis carried out in Sec. III for the linear chain, modified rectangle, and modified cube can be carried forward for any member of the family. Consider the lattice embedded in dimension d . There are 2^d pivotal Green functions $\{x_i\}$ and 2^d recursions. The recursions reduce modulo a point-group symmetry isomorphic to $\oplus_d \mathbb{Z}_2$ yielding a set of symmetry reduced recursions for the symmetrized pivotal set $\{p_i\}$ of the same general form as those for the linear chain, modified rectangle, and modified cube. The canonical variables are of the form

$$a_1 = \frac{p_1 + 1}{p_1 - 1},$$

$$a_i = \frac{(p_1 - 1)(p_i + 1)}{(p_1 + 1)(p_i - 1)} \quad \text{for } i \neq 1. \quad (32)$$

Transforming to the invariant

$$\delta = (a_1)^{2^d} \prod_{i \neq 1}^{2^d} a_i, \quad (33)$$

further reduces the recursions such that

$$\Delta = \delta, \quad (34)$$

and there are $2^d - 1$ residual recursions of the same general form as those for the linear chain, modified rectangle, and modified cube. The diagonal, pivotal Green function in the large lattice limit takes the form

$$x_1 = \frac{(\delta^{(1/2)^d} - 1)}{(\delta^{(1/2)^d} + 1)}, \quad (35)$$

where the initial conditions are determined by computing the Green functions for a d -dimensional hypercube and backing up one step or by computing the Green functions for a $(d-1)$ -dimensional hypercube. In either case, the generation $n=1$ graph is a d -dimensional hypercube.

For the members of the family, the spectral range is $-(d+1) \leq \varepsilon \leq (d+1)$ with dimensionless ground-state energy $(d+1)$. Van Hove singularities exist at $\varepsilon = -(d+1), -(d-1), \dots, -2, 2, \dots, (d-1), (d+1)$ for odd d and $\varepsilon = -(d+1), -(d-1), \dots, -1, 1, \dots, (d-1), (d+1)$ for even d . The bond length between adjacent sites is held fixed for all generations in the recursive construction, leading to a self-similarity dimension $d_f = d$, the Euclidian embedding dimension. The total density of states diverges near the ground-state energy (spectral maximum) as

$$D^{tot}(\varepsilon) \sim |\varepsilon - (d+1)|^{-(1/2)^d},$$

for $\varepsilon \rightarrow (d+1)$. Thus, the spectral dimension as a function of d is

$$d_s = \frac{2^d - 1}{2^{(d-1)}}. \quad (36)$$

Note that $d = d_f > d_s$ and $d_s \rightarrow 2$ as an upper bound as $d \rightarrow \infty$ in agreement with the general result by Hattori *et al.*¹⁸ for coarse-grained fractal structures.

VI. ONE-ELECTRON CONDUCTANCE OF THE MODIFIED RECTANGLE

To address the relationship between electrical conductance and the continuous spectrum and smooth density of states obtained for the modified rectangle lattice, consider the Kubo-Greenwood conductance between one-dimensional leads attached at distal sites of the lattice. The method of calculation is essentially that of Lee and Fisher¹⁹ with suitable modifications.²⁰ Consider two leads formed from disconnected linear chains. The end site k on each chain is connected to the lattice by means of a single bond at attachment sites i and j of the modified rectangle lattice for some generation n . The Green functions before attachment are

$$g_{ii}(z) = g_{jj}(z) \equiv x_n(z),$$

$$g_{ij}(z) = g_{ji}(z) \equiv \begin{cases} y_n(z) \\ u_n(z) \\ v_n(z) \end{cases}, \quad (37)$$

and the Green function at the end of the leads is

$$g_{kk}(z) \equiv \gamma(z) = \frac{z - \sqrt{z-2}\sqrt{z+2}}{2}. \quad (38)$$

The equation for $\gamma(z)$ appearing in Ref. 20 is in error. The present form is correct and in agreement with the result in Eq. (16). The Kubo-Greenwood conductance sum for such a geometry is²⁰

$$c_{ij}(\varepsilon) = 4(\text{Im } \gamma(z))^2 \left| \frac{g_{ij}(z)}{\Delta_{ij}(z)} \right|^2 \quad (39)$$

with

$$\Delta_{ij}(z) = [1 - \gamma(z)x_n(z)]^2 - \gamma(z)^2 g_{ij}(z)^2, \quad (40)$$

and $z = \varepsilon + i\eta$. The conductance as shown in Fig. 8 is quite complicated. In each case there is a distinct transition at $\varepsilon = 1$ (and $\varepsilon = -1$ not shown in the figure) with $c(\varepsilon)$ associated with $y_n(z)$ showing an abrupt transition from nonconducting to conducting behavior as a function of the dimensionless energy. For nonzero η , as $n \rightarrow \infty$ the amplitude decays exponentially $\sim \exp(-L/L_0)$ with lattice diameter $L \sim 2^{n/2}$ as expected.

Starting with initial conditions for dimensionless energy in the range $-1 \leq \varepsilon \leq 1$ and iterating, one finds a one-dimensional attractor shown in Fig. 9 lying in the subspace $d-bc=0$. The properties of the map on this attractor lead to the behavior of the conductance seen in Fig. 8 for $-1 \leq \varepsilon \leq 1$. The attractor can be divided into two one-dimensional rays $b=1, c=d$ and $c=1, b=d$, where $d \in (-\infty, 0]$, that map onto one another under the dynamical system. On this attractor the residual system, Eqs. (22), solves exactly. Let (b_i, c_i, d_i) be an initial point on the attractor. For $b_i = 1$

$$(b_{2m}, c_{2m}) = (1, \tanh^2(2^m \tanh^{-1} \sqrt{c_i})),$$

$$(b_{2m+1}, c_{2m+1}) = (\tanh^2(2^m \tanh^{-1} \sqrt{c_i}), 1), \quad (41)$$

and for $c_i = 1$

$$(b_{2m}, c_{2m}) = (\tanh^2(2^m \tanh^{-1} \sqrt{b_i}), 1),$$

$$(b_{2m+1}, c_{2m+1}) = (1, \tanh^2(2^{m+1} \tanh^{-1} \sqrt{b_i})). \quad (42)$$

On the attractor, $y=0$ leading to the insulating behavior seen in Fig. 8(a) and Eqs. (41) and (42) yield $u_n(z)$ and $v_n(z)$, which alternate between zero and nonzero so that the conductance $c(\varepsilon)$ alternates between zero and some finite value ≤ 1 for fixed ε as a function of n . Thus for $-1 \leq \varepsilon \leq 1$ the conductance is independent of lattice size showing perfect conductance scaling on a set of nonzero measure, behavior that is fundamentally different from the conductance scaling commonly exhibited by regular, hierarchical lattices.^{21,22} For

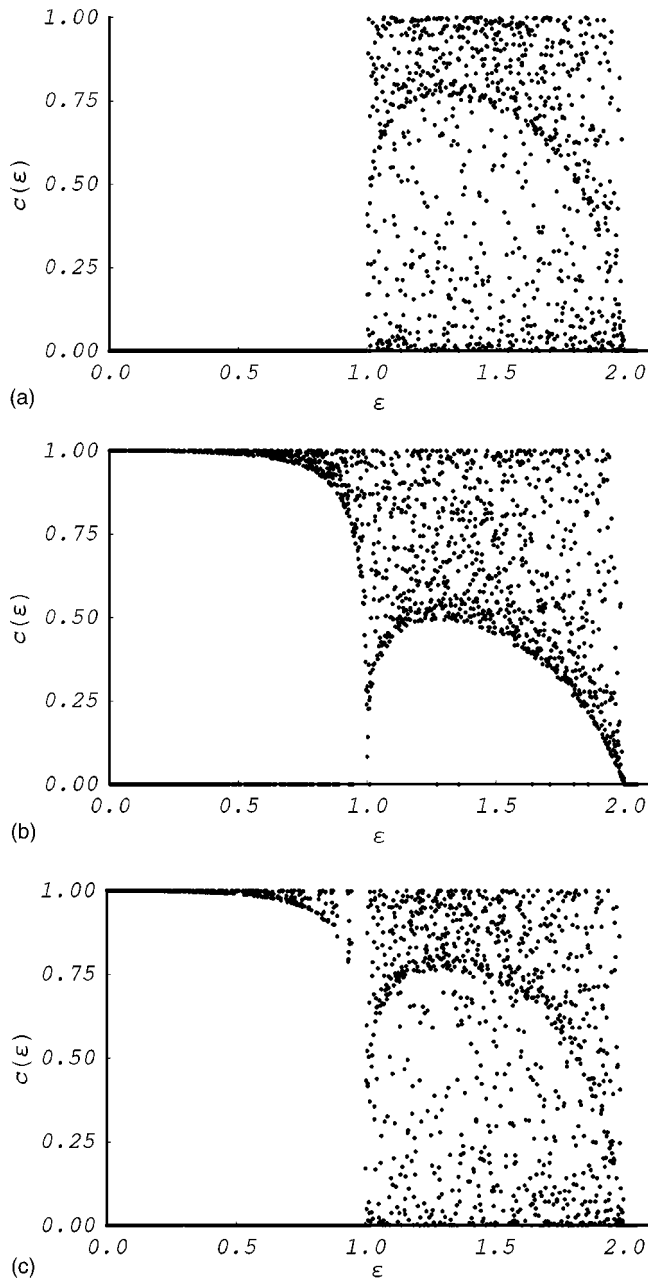


FIG. 8. Kubo-Greenwood conductance in units $e^2/(\pi\hbar)$ between corner sites for $n=4000$ ($\eta=0$). Green functions follow the conventions of Sec. III B and the energy is in units of the hopping matrix element: (a) $c(\epsilon)$ for $g_{ij}(z)=y_n(z)$, (b) $c(\epsilon)$ for $g_{ij}(z)=u_n(z)$, and (c) $c(\epsilon)$ for $g_{ij}(z)=v_n(z)$.

other energies in the spectrum ($-2 \leq \epsilon \leq -1$ and $1 \leq \epsilon \leq 2$) Fig. 8 also shows perfect conductance scaling; however, an analysis similar to that conducted for the interval $-1 \leq \epsilon \leq 1$ has yielded no similar insights.

VII. THE BETHE LATTICE

In a glassy material the chemical bonding requirements tend to keep the coordination constant, resulting in short-range order without long-range order. As one can see from Fig. 1, the vertices of the modified rectangle lattice have a

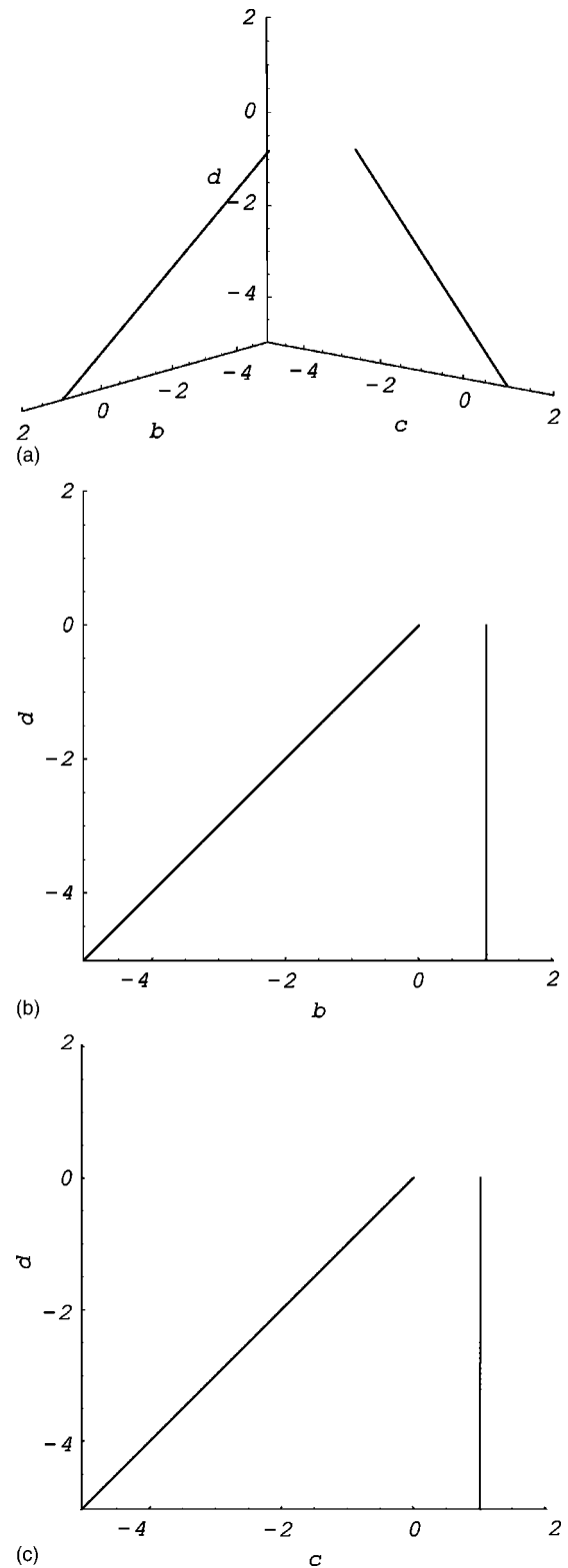
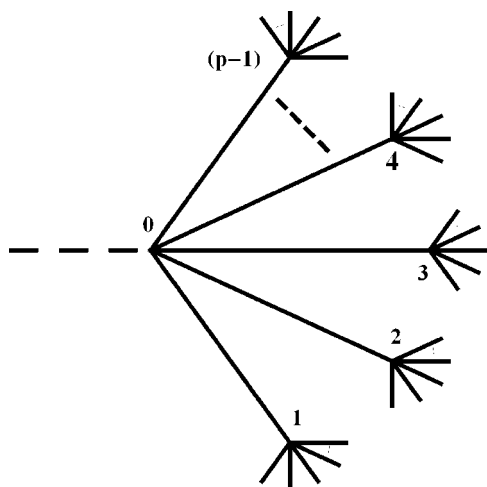


FIG. 9. One-dimensional attractor for $-1 \leq \epsilon \leq 1$: (a) plot of the one-dimensional attractor in the $d-bc=0$ subspace, (b) attractor as viewed in the $b-d$ plane, and (c) attractor as viewed in the $c-d$ plane.

distribution of site environments. The local coordination number is constant, where as a given site is adjacent to three rectangular loops of varying size. This distribution of site environments is shared with typical regular hierarchical lat-

FIG. 10. p -fold coordinated Bethe tree with root site.

tices and differs from regular lattices with translational symmetry in which every site has exactly the same geometric environment in either the infinite-size limit or with periodic boundary conditions. This homogeneity of site environment is also a property of the Bethe lattice. One might try to study the relationship between finite ramification and wave localization, such as Anderson localization, by comparing the spectral and transport properties of the modified rectangle lattice and the Bethe lattice.²³

The Green function $g_o(z)$ for the root site of a p -fold coordinated Bethe tree shown in Fig. 10 found using Eq. (9) is

$$g_o(z) = \frac{z - \sqrt{z-k}\sqrt{z+k}}{2(p-1)}, \quad (43)$$

where the generic off-diagonal Hamiltonian matrix element is 1, $k=2\sqrt{p-1}$, and the sign is chosen so that $g_o(z) \rightarrow 1/z$ as $z \rightarrow \infty$. Connecting two Bethe trees root to root provides an explicit formula for the Green function

$$G_{mn} = A g_o^{|m-n|}, \quad (44)$$

between any two sites m and n in the full Bethe lattice where $|m-n|=l$ is the graph distance and

$$A = \frac{z - p(p-1)g_o}{(z-p)(z+p)}. \quad (45)$$

Since

$$|g_o| = \frac{1}{\sqrt{p-1}}, \quad (46)$$

Eqs. (39), (40), and (44) show that for $p \neq 2$ conductance tends to zero exponentially with distance between the leads.

VIII. CONCLUSION

Taking the family of lattices related to the modified rectangle lattice together with a typical finitely ramified, fractal lattice, such as the 2-simplex lattice, we note that long-range, one-electron conductance does not correlate simply with either the degree of connectivity or the local regularity of the structure. It also seems that no simple correlation exists between conductance and the existence of a spectral continuum as seen from the analysis of the model on the modified rectangle lattice.

The model presented here shows two different properties for a finitely ramified, hierarchical lattice. First, the spectra of the model Hamiltonians turn out to be continuous with a smooth density of states more like that of a regular lattice with translational symmetry and homogeneity of site environments. Second, the modified rectangle exhibits perfect conductance scaling on a set of nonzero measure, which is fundamentally different from the typical behavior of this class of lattice models. In addition, although the spectra are continuous, vanishing conductance or insulating behavior is observed along the diagonal of the modified rectangle on the interval $-1 \leq \varepsilon \leq 1$. The unusual conductance can be explained by the existence of the chaotic attractor and the subsequent analysis of the residual system for the modified rectangle.

*Electronic address: william.schwalm@und.nodak.edu

¹D. Dhar, J. Math. Phys. **18**, 577 (1977).

²D. Dhar, J. Math. Phys. **19**, 5 (1978).

³Y. Gefen, B. Mandelbrot, and A. Aharony, Phys. Rev. Lett. **45**, 855 (1980).

⁴Y. Gefen, A. Aharony, B. Mandelbrot, and S. Kirkpatrick, Phys. Rev. Lett. **47**, 1771 (1981).

⁵W. A. Schwalm and M. K. Schwalm, Phys. Rev. B **39**, 12872 (1989).

⁶P. Anderson, Phys. Rev. **109**, 1492 (1958).

⁷E. Domany, S. Alexander, D. Bensimon, and L. Kadanoff, Phys. Rev. B **28**, 3110 (1983).

⁸R. Rammal, J. Phys. (Paris) **45**, 191 (1984).

⁹C. Domb, Adv. Phys. **9**, 145 (1960).

¹⁰S. Alexander, Phys. Rev. B **29**, 5504 (1984).

¹¹G. R. W. Quispel, J. A. Roberts, and C. J. Thompson, Physica D **34**, 183 (1989).

¹²S. Maeda, Math. Japonica **25**, 405 (1980).

¹³B. Moritz, W. Schwalm, and D. Uherka, J. Phys. A **31**, 7379 (1998).

¹⁴S. Alexander and R. Orbach, J. Phys. (France) Lett. **43**, L625 (1982).

¹⁵R. Rammal and G. Toulouse, J. Phys. (France) Lett. **44**, L13 (1983).

¹⁶S. Havlin and D. Ben-Avraham, Adv. Phys. **36**, 695 (1987).

¹⁷T. Nakayama, K. Yakubo, and R. Orbach, Rev. Mod. Phys. **66**, 381 (1994).

¹⁸K. Hattori, T. Hattori, and H. Watanabe, Phys. Lett. A **115**, 207 (1986).

¹⁹P. A. Lee and D. S. Fisher, Phys. Rev. Lett. **47**, 882 (1981).

²⁰M. K. Schwalm and W. A. Schwalm, Phys. Rev. B **54**, 15086 (1996).

²¹W. A. Schwalm, M. K. Schwalm, and K. G. Rada, Phys. Rev. B **44**, 382 (1991).

²²W. A. Schwalm and M. K. Schwalm, in *Fractals in the Natural and Applied Sciences*, edited by M. M. Novak (Elsevier Science, New York, 1994).

²³J. D. Joannopoulos, Phys. Rev. B **16**, 2764 (1977).